Computational Study on Protolytic Dissociation of HCl and HF in Aqueous Solution

Chang Kon Kim,[†] Byung Ho Park,[†] Chang Kook Sohn, Yu Hee Yu, and Chan Kyung Kim[†,*]

Department of Chemistry Education, Chonnam National University, Gwangju 500-757, Korea
[†]Department of Chemistry, Inha University, Inchon 402-751, Korea. [*]E-mail: kckyung@inha.ac.kr

The protolytic dissociation process of hydrochloric acid (HCl) and hydrofluoric acid (HF) is studied using the B3LYP and MP2 methods with the 6-311+G(d,p) basis set in the gas phase and in aqueous solution. To study the phenomena in detail, discrete and discrete/continuum models were applied by placing water molecules in various positions around the acid. The dissociation process was studied using the thermodynamic cycle involving the structures optimized both in the gas phase and in aqueous solution and was analyzed with two key energy factors, relaxation free energy ($\Delta G_{Rex(g)}$) and solvation free energy (ΔG_s). Based on the results, we could understand the dissociation mechanism and wish to propose the best way to study acid dissociation process using the CPCM methodology in aqueous solution.

Key Words : Dissociation of hydrochloric acid, Dissociation of hydrofluoric acid, CPCM method, Cavity models, Thermodynamic cycle
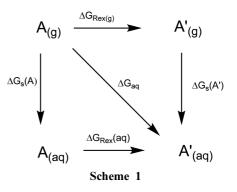
Introduction

The dissociation of an acid in aqueous solution plays a key role in a variety of chemical and biological reactions, and this might be a simple process. However, detailed mechanism for the ionic dissociation of an acid in aqueous solution is difficult to describe at the microscopic molecular level. Especially, one of the problems about mechanism arises from the following question: how many water molecules are directly involved in the dissociation? In nitrogen-matrix study, the HCl-H_2O complex is not ionic but a typical hydrogen-bonded dimer,[1] even if the hydrogen chloride is a strong acid, which dissociated fully in aqueous solution. In argon-matrix studies, Amirand and Maillard found that the ionic dissociation could be described by the clusters of HCl(H_2O)$_n$ with n ≥ 4. These experimental findings were confirmed by several theoretical calculations.[2-8] It is therefore understandable that the ionic dissociation of HCl requires at least four water molecules. However, Chipot and coworkers[9] showed by use of self-consistent reaction field (SCRF) approach that the HCl cluster with two water molecules could dissociate in a moderately polar solution. On the other hand, it was reported that hydrogen fluoride corresponding to a weak acid could not dissociate even in the cluster with five water molecules *in vacuo*.[2] Moreover, there is no evidence of ionic dissociation of HF(H_2O)$_2$ cluster whether the solvent is polar or not. This suggests that the ionic dissociation of hydrogen fluoride might require additional water molecules. Anyway, the general accepted idea is that the acid dissociation in aqueous solution proceeds *via* a cooperative process with some water molecules.

However, most of the previous works focused on the studies in vacuum, even if the bulk solvent effects in the several media were considered in the cases of small clusters of HX (H_2O)$_n$ with n = 1 and 2.[9] The earlier works have concentrated on the stabilities and structures of the clusters, but the complete thermodynamic cycle shown in Scheme 1 was not reported. Therefore, in this work, we examined theoretically the ionic dissociation of acid clusters of HF(H_2O)$_m$ and HCl (H_2O)$_n$, where m = 1-7 and n = 1-5, in the gas phase as well as in aqueous solution by use of the conductor-like Polarizable Continuum Model (CPCM)[10,11] adopting several cavity models.[12,13] As is well known, the continuum model could be one of the popular choices for elucidating the solvent effects, but the main drawback of the model could be the lack of microscopic information such as specific interactions between solute and solvent molecules.[14] Therefore the discrete/continuum solvation model employed in this work could give useful information for specific solvent effects at the microscopic molecular level and bulk solvent effects on the dissociation equilibrium.

In Scheme 1, **A** and **A'** correspond to the optimized structures in the gas phase and in aqueous solution, respectively. ΔG_{Rex} and ΔG_s denote the relaxation energy and solvation energy on going from one structure to another structure, respectively. ΔG_s is the hydration free energy of **A**.

Scheme 1

Computational Details

The equilibrium geometries of $HCl(H_2O)_n$ and $HF(H_2O)_m$ clusters in the gas phase and in aqueous solution were calculated at the B3LYP and MP2 levels with the 6-311+G(d,p) basis set. The bulk solvent effects were considered by use of the CPCM methodology adopting several cavity models. Especially, in this work, to account for the effects of cavity model employed, united atom topological models with implicit hydrogens of UA0 and UAKS models and the cavity models with explicit hydrogens of UFF and Bondi[15] models were examined, because the Gibbs free energies of solvation were largely dependent upon the cavity model employed.[16-18] All the stationary species were fully optimized and characterized by frequency calculations.[19]

To compare the changes in thermochemistry from gas phase to aqueous solution, all the energetics related to structural relaxation and solvation were analyzed in term of the Gibbs free energies as shown in Scheme 1. Especially, in the CPCM method, the non-electrostatic terms are important because the computed energies depend on the cavity size, one of the major components of the non-electrostatic terms.[10-12] Therefore, in this work, the non-electrostatic terms such as cavitation and dispersion were included in the solvation energy terms. Moreover, the Gibbs free energies in aqueous solution, G_{soln}, were obtained by use of Eq. (1), where E_{el}, E_{ZPVE}, E_{Th}, and S are the gas-phase electronic energy, zero-point vibration energy, thermal energy and entropy terms, respectively, calculated on the CPCM optimized structures. The use of gas-phase G_{corr} values on the geometries optimized in solution phase might give better results than the use of G_{corr} values in solution phase as suggested by Ho and co-workers.[18] The last term in Eq. (1) converts the gas-phase standard state to the solution-phase standard state of 1 M. All calculations were performed by using the Gaussian 03 program.[20]

$$G_{soln}(298K) = E_{el} + E_{ZPVE} + E_{Th} + PV - TS + G_s + RT \ln(RT/P)$$
$$= E_{el} + G_{corr} + G_s + RT \ln(RT/P)$$
$$= G_{gas} + G_s + RT \ln(RT/P) \qquad (1)$$

Results and Discussion

To examine the effects of the water clusters, the energetic results on the transferring processes from the gas phase to aqueous solution of the HCl clusters with one and two water molecules are summarized in Tables 1 and 2. As reported in earlier work[9] using the ellipsoidal approximation for the cavity model, dissociation of the clusters with one water molecule, $HCl(H_2O)$, could not take place in aqueous solution condition at all the cavity models employed in this work. However, the dissociation of clusters with two water molecules, $HCl(H_2O)_2$, was largely dependent upon the types of the clusters and theoretical methods employed: The clusters of type (2-i) shown in Scheme 2 dissociated fully at the CPCM-B3LYP level adopting all the cavity models employed. For simplicity, this combination of calculation method and cavity model was abbreviated to CPCM-B3LYP(ALL) and similar notations were used throughout this paper. The bond length of H-Cl, d_{H-Cl}, was 1.287 Å at the B3LYP level in the gas phase, but was elongated to 1.848 Å at the CPCM-B3LYP(UA0) (see Table 1). This result indicates that the cluster of type (2-i) could not dissociate in the gas phase but dissociate in aqueous solution. The clusters of type (2-ii), however, dissociated only at the CPCM-B3LYP(UA0) and CPCM-B3LYP(BONDI).

The clusters of type (2-i) did not dissociate at the CPCM-MP2(UAKS) and CPCM-MP2(UFF), but dissociation occurred at the CPCM-MP2(UA0) and CPCM-MP2(BONDI). Moreover, dissociation of the clusters of type (2-ii) did not take place at the CPCM-MP2(ALL) and at the CPCM-B3LYP(UAKS) and CPCM-MP2(UFF). These results showed that the position of specific water molecule(s) has pro-

Table 1. Calculated bond length (in Å), d_{O-H} and d_{H-Cl}, and the energetics (in kcal mol^{-1}), G_{soln}, $\Delta G_{Rex(g)}$, $\Delta G_s(A')$ and ΔG_{aq}, on transferring $HCl(H_2O)$ and $HCl(H_2O)_2$ clusters from the gas phase to aqueous solution at the CPCM-B3LYP level[a]

Species	Cavity	d_{O-H}	d_{H-Cl}	G_{soln}[b]	$\Delta G_{Rex(g)}$[c]	$\Delta G_s(A')$[d]	ΔG_{aq}[e]	
$HCl(H_2O)$	UA0	1.556	1.365	-537.30480	3.4	-8.0	-4.6	ND
	UAKS	1.633	1.345	-537.30381	2.3	-6.2	-3.9	ND
	UFF	1.630	1.346	-537.29996	2.1	-3.6	-1.5	ND
	BONDI	1.535	1.373	-537.30915	3.6	-10.9	-7.3	ND
$HCl(H_2O)_2$ (2-i)	UA0	1.039	1.848	-613.76997	21.3	-34.5	-13.2	D
	UAKS	1.132	1.648	-613.75642	13.1	-17.9	-4.7	D
	UFF	1.056	1.801	-613.75609	17.5	-22.1	-4.5	D
	BONDI	1.021	1.870	-613.77400	22.2	-38.0	-15.8	D
$HCl(H_2O)_2$ (2-ii)	UA0	1.104	1.694	-613.75352	24.0	-26.9	-2.9	D
	UAKS	1.557	1.364	-613.75385	6.8	-10.0	-3.1	ND
	UFF	1.584	1.358	-613.74727	6.6	-5.6	1.0	ND
	BONDI	1.059	1.814	-613.76450	26.6	-36.4	-9.8	D

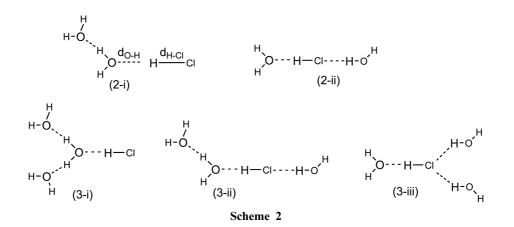[a]**D** and **ND** denote whether the cluster is dissociated or undissociated, respectively. [b]The Gibbs free energy, G_{soln} in hartree, estimated from eq. (1) in aqueous solution. [c]$\Delta G_{Rex(g)} = G(\mathbf{A'}_{(g)}) - G(\mathbf{A}_{(g)})$. [d]$\Delta G_s(A') = G(\mathbf{A'}_{(aq)}) - G(\mathbf{A'}_{(g)})$. [e]$\Delta G_{aq} = G(\mathbf{A'}_{(aq)}) - G(\mathbf{A}_{(g)}) = \Delta G_{Rex(g)} + \Delta G_s(A')$.

Table 2. Calculated bond length (in Å), d_{O-H} and d_{H-Cl}, and the energetics (in kcal mol^{-1}), G_{soln}, $\Delta G_{Rex(g)}$, ΔG_s and ΔG_{aq}, on transferring HCl(H$_2$O) and HCl(H$_2$O)$_2$ clusters from the gas phase to aqueous solution at the CPCM-MP2 level[a]

Species	Cavity	d_{O-H}	d_{H-Cl}	G_{soln}[b]	$\Delta G_{Rex(g)}$[c]	$\Delta G_s(A')$[d]	ΔG_{aq}[e]	
HCl(H$_2$O)	UA0	1.679	1.315	-536.53592	2.5	-10.0	-7.5	ND
	UAKS	1.723	1.307	-536.53329	2.0	-7.8	-5.8	ND
	UFF	1.728	1.307	-536.53107	1.8	-6.2	-4.4	ND
	BONDI	1.717	1.314	-536.53628	2.0	-9.7	-7.7	ND
HCl(H$_2$O)$_2$ (2-i)	UA0	1.042	1.787	-612.81240	27.1	-40.0	-13.0	D
	UAKS	1.641	1.322	-612.80554	4.0	-12.6	-8.7	ND
	UFF	1.639	1.323	-612.80395	1.8	-9.5	-7.7	ND
	BONDI	1.021	1.870	-612.81428	25.9	-40.0	-14.1	D
HCl(H$_2$O)$_2$ (2-ii)	UA0	1.626	1.325	-612.80629	7.0	-16.1	-9.1	ND
	UAKS	1.670	1.316	-612.80249	6.2	-13.0	-6.7	ND
	UFF	1.711	1.311	-612.80184	4.8	-11.2	-6.3	ND
	BONDI	1.677	1.318	-612.81161	5.2	-17.7	-12.5	ND

[a-e]All the footnotes are the same those in Table 1.

Scheme 2

found effects on the dissociation process of the clusters.

To see the effects of additional water molecule(s), three types of the HCl clusters with three water molecules were examined (see Scheme 2) and the energetic results are summarized in Tables 3 and 4. As expected, the clusters of types (3-i) and (3-ii) dissociated fully regardless of the cavity models employed at the CPCM-B3LYP, because protolytic dissociation already occurred in the case of two water molecule cluster, (2-i). The clusters of type (3-iii) showed same trend as the clusters of type (2-ii) at the CPCM-B3LYP(UA0) and CPCM-B3LYP(BONDI). However, at the CPCM-B3LYP (UAKS) and CPCM-B3LYP(UFF) levels, the clusters of type (3-iii) did not dissociate fully, even if d_{H-Cl} was much longer than that in (2-ii). On the other hand, MP2 method showed different dissociation behavior: no dissociation was observed for (3-iii) at the CPCM-MP2(ALL), and also for (3-ii) at the CPCM-MP2(UAKS) and CPCM-MP2(UFF). These results suggest that the water molecule(s) may act favorably for the dissociation of HCl when the water dimer or trimer solvates the hydrogen atom (or proton) not the chloride atom (or anion). In addition, the dissociation of HCl in aqueous solution could be much easier at the B3LYP level than at the MP2 level. At this stage, however, it is not clear which method, B3LYP or MP2, describes this phenomenon

better. Because the clusters of type (3-i) were fully dissociated at all the level of theories considered in this work, the dissociation of HCl in aqueous solution might expect to take place in a cluster with a maximum of three water molecules. Once again, as noted above, the dissociation process of HCl was dependent upon the cavity model employed. However, it is not a matter of the topological model, because protolytic dissociation occurred more in the UA0 (and/or BONDI) model than in the UAKS (and/or UFF) model at both the B3LYP and MP2 methods. In practice, we suggest that the UA0 or UAKS model could be useful for a comparative work, because the calculations adopting the BONDI or UFF were difficult to use because of the convergence problem in many cases.

Examination of Tables 1 and 2 shows that the ΔG_{aq} values for B3LYP and MP2 levels were similar according to the behavior of HCl(H$_2$O) clusters. For example, the ΔG_{aq} values were −3.9 and −5.8 kcal mol^{-1} at the CPCM-B3LYP(UAKS) and CPCM-MP2(UAKS), respectively. It is easy to understand this result because the HCl(H$_2$O) clusters undissociated at all in both the gas phase and aqueous solution. Similarly, the ΔG_{aq} values were also similar for the clusters of type (2-i) at both B3LYP and MP2 levels adopting the UA0 and BONDI cavity models, because the clusters dissociated in

Table 3. Calculated bond length (in Å), d_{O-H} and d_{H-Cl}, and the energetics (in kcal mol^{-1}), G_{soln}, $\Delta G_{Rex(g)}$, ΔG_s and ΔG_{aq}, on transferring HCl(H$_2$O)$_3$ from the gas phase to aqueous solution at the CPCM-B3LYP level[a]

Species	Cavity	d_{O-H}	d_{H-Cl}	G_{soln}[b]	$\Delta G_{Rex(g)}$[c]	$\Delta G_s(A')$[d]	ΔG_{aq}[e]	
HCl(H$_2$O)$_3$ (3-i)	UA0	1.021	1.914	-690.22420	19.3	-34.0	-14.6	D
	UAKS	1.058	1.789	-690.21553	14.8	-24.0	-9.2	D
	UFF	1.027	1.890	-690.21482	14.8	-23.6	-8.7	D
	BONDI	1.009	1.987	-690.23462	18.4	-39.5	-21.2	D
HCl(H$_2$O)$_3$ (3-ii)	UA0	1.033	1.867	-690.21769	23.5	-34.0	-10.5	D
	UAKS	1.085	1.726	-690.20951	17.0	-22.4	-5.4	D
	UFF	1.045	1.831	-690.20330	21.4	-22.9	-1.5	D
	BONDI	1.021	1.940	-690.22621	24.9	-40.7	-15.9	D
HCl(H$_2$O)$_3$ (3-iii)	UA0	1.088	1.723	-690.20346	27.9	-29.5	-1.6	D
	UAKS	1.495	1.384	-690.20289	13.4	-14.6	-1.3	ND
	UFF	1.513	1.379	-690.19771	11.0	-9.0	2.0	ND
	BONDI	1.050	1.835	-690.21842	31.1	-42.1	-11.0	D

[a-e]All of the footnotes are the same in Table 1.

Table 4. Calculated bond length (in Å), d_{O-H} and d_{H-Cl}, and the energetics (in kcal mol^{-1}), G_{soln}, $\Delta G_{Rex(g)}$, ΔG_s and ΔG_{aq}, on transferring HCl(H$_2$O)$_3$ from the gas phase to aqueous solution at the CPCM-MP2 level[a]

Species	Cavity	d_{O-H}	d_{H-Cl}	G_{soln}[b]	$\Delta G_{Rex(g)}$[c]	$\Delta G_s(A')$[d]	ΔG_{aq}[e]	
HCl(H$_2$O)$_3$ (3-i)	UA0	1.025	1.837	-689.08685	21.8	-38.8	-17.1	D
	UAKS	1.067	1.720	-689.07622	17.2	-27.6	-10.4	D
	UFF	1.028	1.829	-689.07975	17.9	-30.5	-12.6	D
	BONDI	1.008	1.923	-689.09337	21.5	-42.7	-21.2	D
HCl(H$_2$O)$_3$ (3-ii)	UA0	1.034	1.808	-689.08430	25.1	-40.6	-15.5	D
	UAKS	1.555	1.341	-689.07558	6.7	-16.7	-10.0	ND
	UFF	1.564	1.340	-689.07255	6.0	-14.1	-8.1	ND
	BONDI	1.023	1.858	-689.08568	26.6	-42.9	-16.3	D
HCl(H$_2$O)$_3$ (3-iii)	UA0	1.568	1.338	-689.07439	12.9	-22.1	-9.2	ND
	UAKS	1.603	1.329	-689.06972	12.2	-18.5	-6.3	ND
	UFF	1.636	1.324	-689.07087	9.5	-16.6	-7.0	ND
	BONDI	1.637	1.327	-689.08568	9.6	-25.9	-16.3	ND

[a-e]All of the footnotes are the same in Table 1.

aqueous solution. For example, the ΔG_{aq} values were −15.8 and −14.1 kcal mol^{-1} at the CPCM-B3LYP(BONDI) and CPCM-MP2(BONDI) levels, respectively. This indicates that the ΔG_{aq} values, *i.e.*, $\Delta G_{Rex}(g)$ and ΔG_s, are similar if the dissociation mechanism is the same, undissociated or dissociated. However, opposite trends were found for (2-i) at both levels adopting the UAKS or UFF cavity models. The clusters dissociated at the CPCM-B3LYP level but undissociated at the CPCM-MP2 level even though the ΔG_{aq} values were not much different (≤ 4 kcal mol^{-1}). For example, the ΔG_{aq} were −4.7 kcal mol^{-1} and −9.6 kcal mol^{-1} at the CPCM-B3LYP(UAKS) and CPCM-MP2(UAKS) levels, respectively. However such a small difference in ΔG_{aq} value seems to be fortuitous, *i.e.*, the favorable ΔG_s and unfavorable $\Delta G_{Rex(g)}$ values at B3LYP level compared to MP2 level were roughly cancelled out, and thus this results in similar ΔG_{aq} values. As summarized in Tables 1 and 2, the ΔG_s at the CPCM-B3LYP(UFF) was more favorable by −12.6 kcal mol^{-1} but the $\Delta G_{Rex(g)}$ was more unfavorable by 15.7 kcal mol^{-1} compared to the corresponding CPCM-MP2 level,

CPCM-MP2(UFF). As a result, the ΔG_{aq} values could roughly become similar for both levels adopting the UAKS and UFF cavity models, even though the transferring processes were different.

To examine the transferring processes for a relatively larger HCl clusters, the HCl(H$_2$O)$_n$ clusters with n = 4-6 were also considered. As reported earlier, the HCl clusters with n $\geq$ 4 dissociated in the gas phase at both B3LYP and MP2 levels. In this work, the geometries of the clusters in aqueous solution were obtained by re-optimizing the gas-phase geometries. The optimized geometries are shown in Figure 1 and the energetics on the transferring processes at the MP2 level of theory are summarized in Table 5. Figure 1 shows that the structure of HCl(H$_2$O)$_4$ cluster in the gas phase was considerably different from the structure in aqueous solution, *i.e.*, in the gas phase, chloride ion was surrounded by two water molecules among the bridged water molecules, but this ion was solvated by only one water molecule in aqueous solution. In contrast, the structures of HCl(H$_2$O)$_5$ and HCl(H$_2$O)$_6$ clusters were very similar both

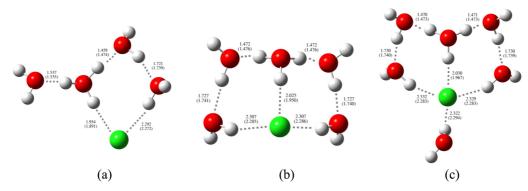   (a)   (b)   (c)

Figure 1. Optimized geometries of the $HCl(H_2O)_n$ clusters. (a) n=4, (b) n=5, and (c) n=6 at the CPCM-B3LYP/6-311+G(d,p) level adopting the UA0 cavity model. Values are in Å, and CPCM-MP2/6-311+G(d,p) values are shown in parentheses.

Table 5. Calculated bond length (in Å), d_{O-H} and d_{H-Cl}, and the energetics (in kcal mol^{-1}), G_{soln}, $\Delta G_{Rex(g)}$, ΔG_s and ΔG_{aq}, on transferring $HCl(H_2O)_n$ with n = 4-6 from the gas phase to aqueous solution at the CPCM-MP2 level[a]

Species	Cavity	d_{O-H}	d_{H-Cl}	G_{soln}[b]	$\Delta G_{Rex(g)}$[c]	$\Delta G_s(A')$[d]	ΔG_{aq}[e]	
$HCl(H_2O)_4$	UA0	1.014	1.891	-765.35918	9.2	-31.1	-21.8	D
	UAKS	1.036	1.807	-765.34943	6.9	-22.7	-15.7	D
	UFF	1.017	1.876	-765.35210	6.2	-23.5	-17.4	D
	BONDI	1.004	1.928	-765.36711	9.4	-36.2	-26.8	D
$HCl(H_2O)_5$	UA0	1.004	1.950	-841.63129	4.7	-24.2	-19.5	D
	UAKS	1.015	1.887	-841.62368	3.2	-17.9	-14.7	D
	UFF	1.005	1.945	-841.62449	3.1	-18.3	-15.2	D
	BONDI	0.998	2.001	-841.64134	4.7	-30.5	-25.8	D
$HCl(H_2O)_6$	UA0	1.001	1.967	-917.90361	6.6	-28.2	-21.6	D
	UAKS	1.008	1.924	-917.89350	5.2	-20.4	-15.2	D
	UFF	1.001	1.967	-917.89687	4.3	-21.7	-17.3	D
	BONDI	0.995	2.014	-917.91685	6.3	-36.2	-29.9	D

[a-e]All of the footnotes are the same in Table 1.

in the gas phase and in aqueous solution. Therefore, geometrical relaxations, $\Delta G_{Rex(g)}$, in $HCl(H_2O)_4$ cluster was larger than those in $HCl(H_2O)_5$ and $HCl(H_2O)_6$ clusters. However, favorable ΔG_s values in $HCl(H_2O)_4$ clusters suggest that the solvating abilities by four water molecules on dissociated species, H^+ and Cl^-, are stronger than those in $HCl(H_2O)_5$ and $HCl(H_2O)_6$ clusters. Consequently, ΔG_{aq} values could become similar for the clusters with n ≥ 4. In other words, contribution of $\Delta G_{Rex(g)}$ to ΔG_{aq} value becomes smaller for larger clusters due to smaller deformation in the structures on going from the gas phase to aqueous phase.

At this point, it would be interesting to examine the role of various Gibbs free energies for the dissociation of HCl clusters from the thermodynamic cycle shown in Scheme 1. One way to do this is to plot ΔG_s against $\Delta G_{Rex(g)}$ using the data in Tables 1-5 (see Figure 2). To distinguish the dissociation phenomena clearly, two different symbols are used to display data in the same table: small and large symbols represent undissociated and dissociated clusters, respectively. Interestingly, the plot can be divided into four quadrants, **(I)-(IV)**. Most of the undissociated clusters are located in **(I)** and all dissociated clusters are in **(III)** and **(IV)**. The clusters belong to **(I)** have smaller $\Delta G_{Rex(g)}$ and $\Delta G_s(A')$ due to neutral character of the clusters. However, the clusters in
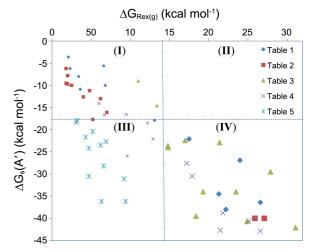

Figure 2. A plot of $\Delta G_s(A')$ *vs.* $\Delta G_{Rex(g)}$ using the data in Tables 1-5. Large and small symbols represent dissociated and undissociated HCl clusters, respectively.

(IV) require large relaxation and solvation free energies because undissociated clusters in the gas phase break down to ionic species in aqueous solution. The clusters belong to **(III)** have smaller relaxation but larger solvation free energies because these species dissociate into ionic species
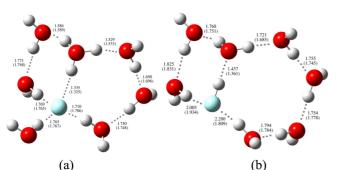
Figure 3. Optimized geometries of HF(H$_2$O)$_7$ cluster. (a) CPCM-B3LYP/6-311+G(d,p). (b) CPCM-MP2/6-311+G(d,p) levels adopting the UA0 cavity model. Values are in Å, and the parentheses values are adopting the UAHF cavity model.

even in the gas phase. Note that there is no data point in (**II**) because such a situation is hard to occur.

Unlike the HCl(H$_2$O)$_n$ clusters discussed above, it was reported that the HF(OH$_2$)$_m$ clusters with m = 1-5 failed to dissociate in the gas phase.[2] Moreover, there is no evidence on the dissociation in the HF(H$_2$O)$_2$ cluster regardless of the solvent polarity.[9] These results could be quite reasonable, because the hydrogen fluoride, HF, is a weak acid. Nevertheless, in this work, we have examined the HF(H$_2$O)$_m$ clusters with m = 1-7 in the gas phase and in aqueous solution to examine how the solvation models behave in this case. The number of water molecules was limited to seven because the first-solvation shell seems to be completed in the HF(H$_2$O)$_7$ cluster (see Figure 3). In aqueous solution, UA0 and UAKS cavity models were selected as noted above in HCl(H$_2$O)$_n$ clusters. Similar to earlier works, all the HF(OH$_2$)$_m$ clusters with m = 1-7 did not dissociate in the gas phase and we expected similar results in aqueous solution. However, HF(H$_2$O)$_7$ cluster dissociated at the CPCM-B3LYP but

undissociated at the CPCM-MP2. Again, this shows that an acid dissociates more easily at the CPCM-B3LYP than at the CPCM-MP2.

Interestingly, CPCM-B3LYP calculation seems to be inadequate in studying the acid dissociation in aqueous solution, because the hydrogen fluoride is a typical weak acid with $K_a = 3.5 \times 10^{-4}$.[21] This implies that the undissociated form could be favorable by $\Delta G = 4.7$ kcal mol^{-1} in the equilibrium process,[22] when compared to the dissociated form. The energetics on the transferring processes of the HF(H$_2$O)$_m$ clusters calculated at the MP2 level of theory are summarized in Table 6. Table 6 shows that the ΔG_s values at the CPCM-MP2(UA0) are 4-6 kcal mol^{-1} more favorable, but the ΔG_{Rex}(g) values at the same level of theory are 1-4 kcal mol^{-1} unfavorable for m ≥ 3 when compared to the corresponding data obtained at the CPCM-MP2(UAKS). Consequently, the ΔG_{aq} values at CPCM-MP2(UA0) are always 4-5 kcal mol^{-1} lower than those at the CPCM-MP2(UAKS). If the data in Table 6 are displayed in Figure 2, all the points can be found in (**I**) and (**III**), which have small relaxation but larger solvation free energies as the number of water molecules increases.

To investigate ionic dissociation process of HF in aqueous solution, a hypothetical dissociation process, Eq. (2), was examined for HF(H$_2$O)$_m$ clusters with m ≥ 4. In Eq. (2), the hydronium is described as (H$_2$O)$_3$H$^+$$_{(aq)}$ because the hydronium ion in solution has a well-defined first solvation shell with three water molecules.[23] The Gibbs free energies of dissociation, ΔG_D, are summarized in Table 7. The ΔG_D value becomes more favorable as the number of water molecules increases at the CPCM-MP2(UA0) and this value approaches experimental value[22] of 4.7 kcal mol^{-1} as the number of water molecules increases. But no such trend was observed in the case of CPCM-MP2(UAKS). This suggests that CPCM-MP2(UA0) might be the best method in studying

Table 6. Calculated bond length (in Å), d_{O-H} and d_{H-F}, and the energetics (in kcal mol^{-1}), G_{soln}, ΔG_{Rex}(Gas), ΔG_s and ΔG_{aq}, on transferring HF(H$_2$O)$_m$ clusters with m = 1-7 from the gas phase to aqueous solution at the CPCM-MP2 level[a]

m	Cavity	d_{O-H}	d_{H-F}	G_{soln}[b]	$\Delta G_{Rex(g)}$[c]	ΔG_s(A')[d]	ΔG_{aq}[e]
1	UA0	1.564	0.954	-176.57401	2.0	-12.4	-10.3
	UAKS	1.576	0.952	-176.57167	1.8	-10.6	-8.9
2	UA0	1.509	0.966	-252.84861	4.7	-18.8	-14.1
	UAKS	1.537	0.960	-252.84428	3.9	-15.3	-11.4
3	UA0	1.474	0.975	-329.12281	5.9	-23.5	-17.5
	UAKS	1.503	0.967	-329.11753	4.9	-19.1	-14.2
4	UA0	1.445	0.986	-405.39244	3.6	-20.1	-16.5
	UAKS	1.456	0.982	-405.38703	2.8	-15.9	-13.1
5	UA0	1.410	0.999	-481.66237	4.2	-18.8	-14.6
	UAKS	1.405	1.001	-481.65687	3.5	-14.6	-11.1
6	UA0	1.371	1.014	-557.93674	4.4	-20.8	-16.4
	UAKS	1.368	1.016	-557.93093	3.7	-16.4	-12.7
7	UA0	1.437	0.988	-634.20712	7.4	-25.8	-18.3
	UAKS	1.361	1.018	-634.20314	3.9	-19.7	-15.8

[a]All the clusters were not dissociated. [b-e]All of the footnotes are the same in Table 1.

Table 7. The calculated energetic on the dissociation processes, eq. (2), in aqueous solution at the CPCM-MP2 level of theory

Cavity	m	$G_{soln}[HF(H_2O)_n]^a$	$G_{soln}[(H_2O)_{m-3}F^-]^a$	$\Delta G_D{}^b$
UA0	4	-405.39244	-176.11789	13.9
	5	-481.66237	-252.39216	11.2
	6	-557.93674	-328.67007	9.0
	7	-634.20712	-404.94256	7.7
UAKS	4	-405.38703	-176.12537	17.8
	5	-481.65687	-252.39688	16.7
	6	-557.93093	-328.66849	18.3
	7	-634.20314	-404.93919	19.2

^{a}Values were estimated by eq. (1) in hartree. $^b\Delta G_D = \{G_{soln}[(H_2O)_{m-3}F^-] + G_{soln}[(H_2O)_3H^+]\} - G_{soln}[HF(H_2O)_m]$ in kcal mol^{-1}. The $G_{soln}[(H_2O)_3H^+]$ values were estimated to be −229.25234 and −229.23335 H at the CPCM-MP2(UA0) and CPCM-MP2(UAKS) levels, respectively.

acid dissociation processes.

$$HF(H_2O)_{m(aq)} \rightarrow (H_2O)_3H^+{}_{(aq)} + (H_2O)_{m-3}F^-{}_{(aq)} \qquad (2)$$

Conclusion

In this work, we studied dissociation of HCl and HF using discrete solvent model in the gas phase and discrete/continuum model in aqueous solution. All the structures were fully minimized at the B3LYP and MP2 levels of theory with the 6-311+G(d,p) basis set. Four different cavity models were examined in aqueous solution. In the case of HCl, the position of water molecule(s) is an important factor for dissociation, especially water molecule(s) positioned near to the hydrogen atom. At least three water molecules are required for dissociation. In the case of HF, no dissociation took place until seven water molecules are in close proximity to the weak acid except one case. From this work, we found that analysis based on thermodynamic cycle can give us unique insight into the dissociation mechanism and the most promising solvation model might be CPCM-MP2 combined with UA0 cavity model in terms of accuracy and reliability of the results.

References

1. Ault, B. S.; Pimentel, G. C. *J. Phys. Chem.* **1973**, *77*, 57.
2. Cabaleiro-Lago, E. M.; Hermida-Ramón, J. M.; Rodríguez-Otero, J. *J. Chem. Phys.* **2002**, *117*, 3160.
3. Milet, A.; Struniewicz, C.; Moszynski, R.; Wormer, P. E. S. *J. Chem. Phys.* **2001**, *115*, 349.
4. Lee, C.; Sosa, C.; Planas, M.; Novoa, J. J. *J. Chem. Phys.* **1996**, *104*, 7081.
5. Planas, M.; Lee, C.; Novoa, J. J. *J. Phys. Chem.* **1996**, *100*, 16495.
6. Re, S.; Osamura, Y.; Suzuki, Y.; Schaefer, H. F., III. *J. Chem. Phys.* **1998**, *109*, 973.
7. Smith, A.; Vincent, M. A.; Hillier, I. H. *J. Phys. Chem. A* **1999**, *103*, 1132.
8. Bacelo, D. E.; Binning, R. C., Jr.; Ishikawa, Y. *J. Phys. Chem. A* **1999**, *103*, 4631.
9. Chipot, C.; Gorb, L. G.; Rivail, J. L. *J. Phys. Chem.* **1994**, *98*, 1601.
10. Cossi, M.; Rega, N.; Scalmani, G.; Barone, V. *J. Comput. Chem.* **2003**, *24*, 669.
11. Barone, V.; Cossi, M.; Tomasi, J. *J. Comput. Chem.* **1998**, *19*, 404.
12. Takano, Y.; Houk, K. N. *J. Chem. Theo. Comput.* **2005**, *1*, 70.
13. Tomasi, J.; Mennucci, B.; Cammi, R. *Chem. Rev.* **2005**, *105*, 2999.
14. Spoviero, E. M.; Newcomer, M. B.; Gascón, J. A.; Bastista, E. R.; Brudvig, G. W.; Batista, V. S. *Photosynth. Res.* **2009**, *102*, 455.
15. Bondi, A. *J. Phys. Chem.* **1964**, *68*, 441.
16. Kim, C. K.; Park, B.-H.; Lee, H. W.; Kim, C. K. *Bull. Korean Chem. Soc.* **2011**, *32*, 1985.
17. Kim, C. K.; Park, B.-H.; Lee, H. W.; Kim, C. K. *Org. Biomol. Chem.* **2013**, *11*, 1407.
18. Ho, J.; Klamt, A.; Coote, M. L. *J. Phys. Chem. A* **2010**, *114*, 13442.
19. Some optimized structures had one or more small imaginary frequencies in Gaussian 03 calculations. But these frequencies disappeared when the structures were re-optimized using Gaussian 09 package. See Arstad, B.; Blom, R.; Swang, O. *J. Phys. Chem. A* **2007**, *111*, 1222.
20. Gaussian 03, Revision B.05, Frisch, M. J.; Trucks, G. W.; Schlegel, H. B.; Scuseria, G. E.; Robb, M. A.; Cheeseman, J. R.; Montgomery, J. A., Jr.; Vreven, T.; Kudin, K. N.; Burant, J. C.; Millam, J. M.; Iyengar, S. S.; Tomasi, J.; Barone, V.; Mennucci, B.; Cossi, M.; Scalmani, G.; Rega, N.; Petersson, G. A.; Nakatsuji, H.; Hada, M.; Ehara, M.; Toyota, K.; Fukuda, R.; Hasegawa, J.; Ishida, M.; Nakajima, T.; Honda, Y.; Kitao, O.; Nakai, H.; Klene, M.; Li, X.; Knox, J. E.; Hratchian, H. P.; Cross, J. B.; Bakken, V.; Adamo, C.; Jaramillo, J.; Gomperts, R.; Stratmann, R. E.; Yazyev, O.; Austin, A. J.; Cammi, R.; Pomelli, C.; Ochterski, J. W.; Ayala, P. Y.; Morokuma, K.; Voth, G. A.; Salvador, P.; Dannenberg, J. J.; Zakrzewski, V. G.; Dapprich, S.; Daniels, A. D.; Strain, M. C.; Farkas, O.; Malick, D. K.; Rabuck, A. D.; Raghavachari, K.; Foresman, J. B.; Ortiz, J. V.; Cui, Q.; Baboul, A. G.; Clifford, S.; Cioslowski, J.; Stefanov, B. B.; Liu, G.; Liashenko, A.; Piskorz, P.; Komaromi, I.; Martin, R. L.; Fox, D. J.; Keith, T.; Al-Laham, M. A.; Peng, C. Y.; Nanayakkara, A.; Challacombe, M.; Gill, P. M. W.; Johnson, B.; Chen, W.; Wong, M. W.; Gonzalez, C.; Pople, J. A. Gaussian, Inc., Wallingford, CT, 2003.
21. Atkins, P.; Jones, L. In *Chemical Principles, The Quest for Insight*; W. H. Freeman and Company: New York, USA, 2005; p 376.
22. The ΔG value was estimated by use of ΔG = −RT ln K at 298 K.
23. Tuñón, I.; Silla, E.; Bertrán, J. *J. Phys. Chem.* **1993**, *97*, 5547.